

**Aqueous phase
processing of
secondary organic
aerosols**

Y. Liu et al.

Aqueous phase processing of secondary organic aerosols

Yao Liu¹, T. Tritscher², A. P. Praplan², P. F. DeCarlo^{2,*}, B. Temime-Roussel¹,
E. Quivet¹, N. Marchand¹, J. Dommen², U. Baltensperger², and A. Monod¹

¹Université Aix-Marseille I, II et III, Case 29, UMR6264, CNRS – Laboratoire Chimie
Provence, 3 place Victor Hugo, 13331 Marseille Cedex 3, France

²Paul Scherrer Institut (PSI), Laboratory of Atmospheric Chemistry, 5232 Villigen, Switzerland

* now at: AAAS Science and Technology Policy Fellow Hosted at the US EPA,
Washington, DC, USA

Received: 22 July 2011 – Accepted: 25 July 2011 – Published: 28 July 2011

Correspondence to: A. Monod (anne.monod@univ-provence.fr)

Published by Copernicus Publications on behalf of the European Geosciences Union.

Title Page

Abstract

Introduction

Conclusions

References

Tables

Figures

⏪

⏩

◀

▶

Back

Close

Full Screen / Esc

Printer-friendly Version

Interactive Discussion

Abstract

The aging of secondary organic aerosol (SOA) by photooxidation in the aqueous phase was experimentally investigated. To simulate multiphase processes, the following experiments were sequentially performed in a smog chamber and in an aqueous phase photoreactor: (1) Gas-phase photooxidation of three different volatile organic compounds (VOC): isoprene, α -pinene, and 1,3,5-trimethylbenzene (TMB) in the presence of NO_x , leading to the formation of SOA which was subjected to on-line physical and chemical analysis; (2) particle-to-liquid transfer of water soluble species of SOA using filter sampling and aqueous extraction; (3) aqueous-phase photooxidation of the obtained water extracts; and (4) nebulization of the solutions for a repetition of the on-line characterization. SOA concentrations in the chamber measured with a scanning mobility particle sizer (SMPS) were higher than $200 \mu\text{g m}^{-3}$, as the experiments were conducted under high initial concentrations of volatile organic compounds (VOC) and NO_x . The aging of SOA through aqueous phase processing was investigated by measuring the physical and chemical properties of the particles online before and after processing using a high resolution time-of-flight aerosol mass spectrometer (AMS) and a hygroscopicity tandem differential mobility analyzer (H-TDMA). It was shown that, after aqueous phase processing, the particles were significantly more hygroscopic, and contained more fragmentation ions at $m/z = 44$ and less ions at $m/z = 43$, thus showing a significant impact on SOA aging for the three different precursors. Additionally, the particles were analyzed with a thermal desorption atmospheric pressure ionization aerosol mass spectrometer (TD-API-AMS). Comparing the smog chamber SOA composition and non processed nebulized aqueous extracts with this technique revealed that sampling, extraction and/or nebulization did not significantly impact the chemical composition of SOA formed from isoprene and α -pinene, whereas it affected that formed from TMB. For the two first precursors, the aqueous phase chemical composition of SOA was further investigated using offline measurements, i.e. ion chromatography coupled to a mass spectrometer (IC-MS) and an atmospheric pressure

Aqueous phase processing of secondary organic aerosols

Y. Liu et al.

Title Page

Abstract

Introduction

Conclusions

References

Tables

Figures

⏪

⏩

◀

▶

Back

Close

Full Screen / Esc

Printer-friendly Version

Interactive Discussion



chemical ionization mass spectrometer (APCI-MS) equipped with high pressure liquid chromatography (HPLC-MS). These analyses showed that aqueous phase processing enhanced the formation of some compounds already present in the SOA, thus confirming the aging effect of aqueous phase processes. For isoprene experiments, additional new compounds, likely oligomers, were formed through aqueous phase photooxidation, and their possible origins are discussed.

1 Introduction

Secondary organic aerosol (SOA), formed by the chemical transformation of atmospheric organic compounds, accounts for a large, and often a dominant fraction of total organic aerosol (Hallquist et al., 2009). More than 50 % of the total organic aerosol mass can be attributed to SOA (Zhang et al., 2005; Lanz et al., 2007; Jimenez et al., 2009). Detailed knowledge of the formation, characterization, and fate of SOA is required to evaluate its impact on atmospheric processes, climate and human health. The chemical characterization of SOA shows the presence of oxygenated and water soluble organic compounds such as carbonyl species, acids, esters, alcohols as well as polymers or oligomers (Tolocka et al., 2004; Kalberer et al., 2004; Kourtchev et al., 2005; Edney et al., 2005; Baltensperger et al., 2005; Dommen et al., 2006; Surratt et al., 2006; Müller et al., 2008; Healy et al., 2008; Hallquist et al., 2009). The atmospheric oxidation of these organic particles affects the physical and chemical properties of aerosols through a process known as aging. The most recent studies on aging of organic aerosol have focused on heterogeneous reactions, condensation, volatilization, as well as changes in hygroscopicity, O:C ratio (oxygen to carbon molar ratio), and density (Rudich et al., 2007; Kroll et al., 2008; Jimenez et al., 2009; Tritscher et al., 2011).

A fraction of the numerous organic compounds encountered in atmospheric water droplets (Kawamura et al., 1999, 2001; Sorooshian et al., 2007a,b; Hua et al., 2008) is likely coming from both the gas phase and water dissolution of the organic matter

Aqueous phase processing of secondary organic aerosols

Y. Liu et al.

Title Page

Abstract

Introduction

Conclusions

References

Tables

Figures

⏪

⏩

◀

▶

Back

Close

Full Screen / Esc

Printer-friendly Version

Interactive Discussion



present in the initial condensation nuclei (van Pinxteren et al., 2005; Hallquist et al., 2009). Clouds continuously appear and disappear through evapo-condensation cycles, thus inducing continuous re-partitioning of organic compounds between the gas, aqueous, and particle phases. It is known that the reactivity of organic compounds can be very different in the aqueous phase compared to the gas phase (Altieri et al., 2006, 2008; Carlton et al., 2007; Liu et al., 2009; El Haddad et al., 2009; Poulain et al., 2010; Sun et al., 2010). Therefore, it is possible that the aging of SOA through evapo-condensation cycles of clouds results in very different physical and chemical composition than the aging in the gas phase alone. A number of recent studies have focused on the ability of aqueous phase reactivity of some single organic compounds with OH radical to form oligomers, and potentially new SOA (Altieri et al., 2006, 2008; Carlton et al., 2006, 2007; Perri et al., 2009; El Haddad et al., 2009; Tan et al., 2009, 2010; Zhang et al., 2010; Liu et al., 2011). However, the effects of aqueous phase photooxidation of a complex mixture of organic compounds, such as those encountered in SOA, have only very recently been experimentally investigated by a few authors (Lee et al., 2011; Bateman et al., 2011) who have shown that this type of approach reveals a number of new aspects of SOA aging, that can be more atmospherically representative than the classical dry heterogeneous reactivity.

The aim of this study was to investigate the aging of different types of SOA by photooxidation in the aqueous phase. In order to control the origin of the SOA, we produced SOA through smog chamber photochemical experiments from three different precursors: isoprene, α -pinene and 1,3,5-trimethylbenzene (TMB).

2 Experimental section

2.1 General overview

The aging of SOA during evapo-condensation cycles of a cloud was investigated under simulated conditions using a smog chamber and an aqueous phase photoreactor.

Aqueous phase processing of secondary organic aerosols

Y. Liu et al.

Title Page

Abstract

Introduction

Conclusions

References

Tables

Figures



Back

Close

Full Screen / Esc

Printer-friendly Version

Interactive Discussion



**Aqueous phase
processing of
secondary organic
aerosols**

Y. Liu et al.

Title Page

Abstract

Introduction

Conclusions

References

Tables

Figures

⏪

⏩

◀

▶

Back

Close

Full Screen / Esc

Printer-friendly Version

Interactive Discussion



Figure 1 illustrates the experimental set-up. SOA formed by the gas-phase photooxidation of isoprene, α -pinene or TMB was generated in the smog chamber, under the conditions presented in Table 1. In order to obtain large quantities of SOA, high initial concentrations of VOCs and NO_x were used at room temperature and a relative humidity of about 50 %. The formed particles were collected on filters at 6 l min^{-1} during 2 h, and extracted by sonication of the filters in ultra-high quality (UHQ) water (Millipore). The extracted solution was then separated into three samples (Fig. 1): (i) “ $\text{H}_2\text{O}_2 + h\nu$ ” sample: 100 ml of the solution was placed in an aqueous phase photoreactor to undergo photooxidation with OH radicals during 20 hours. OH radicals were generated in situ by the photolysis of hydrogen peroxide (H_2O_2), which was added to the solution prior to photolysis, in concentrations indicated in Table 1. (ii) “Dark H_2O_2 ” sample: H_2O_2 was added to 30 ml of the extracted solution and kept in the dark, in order to compare the effects of H_2O_2 with those of OH radicals. (iii) “control” sample: 30 ml of the solution was left in the dark during the same time as the two other samples, in order to check for reactive changes of the untreated solution, compared to its reactivity towards H_2O_2 and/or OH radicals. In order to simulate a cloud evaporation process, each of the above mentioned solution was then nebulized with an atomizer. The aerosol before and after the cloud simulation processes was analyzed with a suite of instruments as specified below. Four experiments are presented here in Table 1: two experiments with isoprene, one with α -pinene and one with TMB. The instruments used for these experiments are described hereafter.

2.2 Analysis

2.2.1 On-line aerosol characterization

The physical and chemical characterization of the SOA was performed online in the smog chamber and after their aqueous phase processing and subsequent nebulization using the following instruments.

SMPS: scanning mobility particle sizer

A condensation particle counter (CPC, TSI 3025A) monitored the evolution of the total aerosol particle number concentration. The number size distribution was measured with a scanning mobility particle sizer (SMPS) consisting of a differential mobility analyzer (DMA, TSI 3071) and a CPC (TSI 3022A).

H-TDMA: hygroscopicity tandem differential mobility analyzer

The custom built H-TDMA selects a dry, narrow size fraction of the aerosol (DMA1), humidifies it at high relative humidity (RH 90 %) and scans the conditioned aerosol with a second DMA (DMA2) and a CPC (TSI 3022A). The used instrument is described in Tritscher et al. (2011). From the measured size distribution a hygroscopic growth factor for a certain RH is calculated. The H-TDMA data were calibrated, analyzed and inverted with the TDMA_{inv} procedure from Gysel et al. (2009). Measured dry particle diameters ranged from 35–150 nm during the nebulizer experiments. To exclude the Kelvin effect we present the data in the form of the hygroscopicity parameter κ (Petters and Kreidenweis, 2007), assuming the surface tension of pure water. κ ranges from 0 for insoluble, but wettable material to ca. 1.4 for very hygroscopic salts.

AMS

A high resolution time-of-flight aerosol mass spectrometer (DeCarlo et al., 2006) was used to measure online the bulk chemical composition of the non-refractory submicron particulate matter. Data was saved every two minutes during smog chamber experiments and during nebulization.

Aqueous phase processing of secondary organic aerosols

Y. Liu et al.

Title Page

Abstract

Introduction

Conclusions

References

Tables

Figures

⏪

⏩

◀

▶

Back

Close

Full Screen / Esc

Printer-friendly Version

Interactive Discussion



TD-API-AMS: thermal desorption atmospheric pressure ionization aerosol mass spectrometer

Further on-line analysis of the chemical composition of SOA was performed using a modified version of a commercial (Varian 1200L) atmospheric pressure chemical ionization device, equipped with a triple quadrupole mass spectrometer (APCI-MS/MS). The inlet of this instrument has been modified to transform it into an aerosol mass spectrometer, named TD-API-AMS, as described and validated by Eyglunent et al. (2008). Briefly, the modified inlet consists of a charcoal denuder (to trap gas phase VOCs and semi-volatile organic compounds) followed by a modified thermal-desorption unit (held at 300 °C) attached to the APCI source. The aerosol was injected at a flow rate of 2 l min⁻¹. In order to optimize the ionization, liquid methanol (10 μl min⁻¹) was continuously vaporized in the air stream containing the volatilized organic aerosol prior to ionization by a corona discharge. The intensity of the corona discharge was set at 9 μA and the shield voltage at 600 V. The analyses were performed using alternatively the positive and the negative ionization modes with a capillary voltage of +40 V and -40 V, respectively. Nitrogen served both as the drying gas and the auxiliary gas was delivered at a pressure of 1.0 × 10⁵ and 1.4 × 10⁴ Pa, respectively. The drying gas temperature was held at 350 °C. The total ion current (TIC) of the mass spectra were recorded between 65 and 1000 Da (Dalton) for the negative mode, and between 59 and 1000 Da for the positive mode during the analysis, with a resolution of 1.0 Da and a scan time of 5 s. This instrument is complementary to the AMS as the atmospheric pressure chemical ionization is a soft ionization method resulting in minimal fragmentation, and thus it allows one to determine the molar mass of most of the compounds present in the mixture. In positive ionisation, ions are produced by protonation with H⁺ or cationization with sodium ions (Na⁺, present in all glasswares, and in particular in the syringe bringing methanol into the air stream), leading to [M + 1]⁺ or [M + 23]⁺ ions for most oxygenated compounds. Negative ionization mode leads to formation of deprotonated ions [M - 1]⁻ and gives a response primarily for species bearing an acidic hydrogen.

Aqueous phase processing of secondary organic aerosols

Y. Liu et al.

Title Page

Abstract

Introduction

Conclusions

References

Tables

Figures

⏪

⏩

◀

▶

Back

Close

Full Screen / Esc

Printer-friendly Version

Interactive Discussion



2.2.2 Aqueous phase characterizations

The chemical composition of liquid samples before and after 20 h of reaction with OH, or H₂O₂, or untreated, was analyzed by an atmospheric pressure chemical ionization mass spectrometer operated with either a direct infusion of the solutions (APCI-MS), or with a liquid chromatographic separation column (HPLC-APCI-MS), and ion chromatography coupled to a mass spectrometer (IC-MS).

APCI-MS and APCI-MS²

Direct analysis of the liquid samples was performed using the APCI-MS and APCI-MS². Samples and standard solutions were directly injected into the APCI source (no chromatographic column) at a flow rate of 40 μl min⁻¹. In order to optimize the ionization of organic molecules, liquid methanol (0.2 μl min⁻¹) was continuously vaporized into the APCI source using an HPLC pump. The nebulizing gas was nitrogen for the positive mode and synthetic air for the negative mode, delivered at a pressure of 55 psi at 300 °C. All other parameters (i.e. voltages, pressures and temperatures of drying and auxiliary gases, corona discharge intensity and voltage, mass range, resolution and scan time) were set at the same conditions as those indicated above for the TD-API-AMS analyses. The compounds were identified by APCI-MS² characterization. In this case, argon (collision gas) was delivered at a pressure of 0.27 Pa to the collision cell. The collision energy was between 5 and 20 V depending on the compound, with a resolution of 1.0 Da and a scan time of 0.5 s.

HPLC-APCI-MS

Liquid samples generated during the experiments with isoprene were also analyzed by HPLC-APCI-MS. The separation column was a synergi Hydro-RP 250 × 2.4 μm, phenomenex. The analytes were subjected to chromatography using a gradient of two solvents (A: 0.1 % acetic acid aqueous solution and B: methanol) delivered at a constant

Aqueous phase processing of secondary organic aerosols

Y. Liu et al.

Title Page

Abstract

Introduction

Conclusions

References

Tables

Figures

⏪

⏩

◀

▶

Back

Close

Full Screen / Esc

Printer-friendly Version

Interactive Discussion



flow rate of 0.2 ml min^{-1} . The elution program was: 5 % of B from 0 to 12 min, then increased to 100 % from 12 min to 60 min, followed by 100 % of B from 60 to 65 min, and 5 % B until 90 min. The analyses were realized using single ion monitoring (SIM) in the positive and in the negative mode. The APCI parameters were the same as described above with a resolution of 1.0 Da and a scan time of 0.5 s.

IC-MS

Liquid samples were also analyzed by IC-MS, in order to detect the organic acids present in the extracts. The samples were directly injected onto a separation column (AS11-HC with guard column AG-11HC, Dionex) where they were eluted within 29 min with a hydroxy anion (OH^-) gradient: 0 min 0.5 m M OH^- , 5 min 0.5 m M, 15 min 20 m M, 21 min 60 m M, 23 min 60 m M, 23.1 min 0.5 m M, 29 min 0.5 m M. After elution, the OH^- was eliminated by an anion self-regenerating suppressor (ASRS[®] Ultra 2mm, Dionex). The detector was a mass spectrometer coupled with an electrospray ionization source (ESI-MS) operated in the negative mode, with a capillary voltage of 3.5 kV and a source voltage of 50 V. The nebulizing gas was held at 450°C . The acids were identified by their m/z values and their retention times (RT), by comparison to commercially available standards.

2.3 Chamber experiments

The Paul Scherrer Institute smog chamber has been described in detail elsewhere (Paulsen et al., 2005). Briefly, it is a 27-m^3 Teflon bag ($3 \text{ m} \times 3 \text{ m} \times 3 \text{ m}$) enclosed in a thermally regulated housing. The chamber is illuminated with four 4-kW xenon arc lamps, to simulate the tropospheric solar spectrum. The lights are turned on after the gaseous precursors are equilibrated in the chamber (typically 15–30 min). Experiments were monitored with a variety of aerosol and gas-phase characterization instruments, as outlined above. All experiments were conducted at 50–60 % relative humidity, and no seed particles were added in any experiment.

21497

ACPD

11, 21489–21532, 2011

Aqueous phase processing of secondary organic aerosols

Y. Liu et al.

Title Page

Abstract

Introduction

Conclusions

References

Tables

Figures

⏪

⏩

◀

▶

Back

Close

Full Screen / Esc

Printer-friendly Version

Interactive Discussion



2.4 Aqueous phase experiments

OH-oxidation of the water extracts was performed in an aqueous phase photoreactor described in detail in Monod et al. (2005, 2000). Briefly, it is a Pyrex thermo-controlled reactor of 450 cm³, equipped with a xenon arc lamp (300 W; Oriel), and a pyrex filter to remove the UV irradiation below 300 nm. The resulting irradiance spectrum was comparable to the one of the sun at the earth's ground level (in the UV-visible region), but much less intense (about 4 %). H₂O₂ was added to the water extracts prior to photolysis, in order to produce OH radicals. The aqueous solution was continuously stirred and maintained at a constant temperature (298 ± 0.2 K). The initial H₂O₂ concentrations were chosen in order to produce sufficient quantities of OH radicals in the aqueous phase to oxidize the extracted organic compounds from the SOA. The initial concentrations of H₂O₂ were calculated (i) using estimated values of the aqueous phase concentrations of soluble organic compounds; (ii) assuming for them an aqueous phase OH-oxidation rate constant similar to the one of methacrolein (Liu et al., 2009) (for isoprene experiments), and pinic acid (calculated using the Structure-Activity Relationship – SAR – of Monod and Doussin, 2008) (for α -pinene and TMB experiments); and (iii) in order to favour the OH-oxidation of soluble organics rather than that of H₂O₂ by a factor of more than 70 % (under the above assumptions).

2.5 Nebulization experiments

Liquid solutions were nebulized using a TSI 3076 type nebulizer, and an experimental set up described in details in Paulsen et al. (2006). The particle laden air out of the nebulizer, with a flow of ~1.5 l min⁻¹, was diluted by synthetic air with a flow of ~1.5 l min⁻¹ from a gas bottle or a pure air generator (AADCO Instruments, Inc., USA, 737-250 series).

For all of experiments described here (No. 1 to 4, see Table 1), the “control”, “dark H₂O₂” and “H₂O₂ + h ν ” samples were nebulized during at least 90 min. During nebulization, the total organic aerosol mass (measured by the AMS) showed a positive or

Aqueous phase processing of secondary organic aerosols

Y. Liu et al.

[Title Page](#)[Abstract](#)[Introduction](#)[Conclusions](#)[References](#)[Tables](#)[Figures](#)[⏪](#)[⏩](#)[◀](#)[▶](#)[Back](#)[Close](#)[Full Screen / Esc](#)[Printer-friendly Version](#)[Interactive Discussion](#)

5 a negative time trend. The reason for this variability is not clear but, in some cases, it may be due to changes in the chemical composition during nebulization (see Sect. 3.3). Relative measured parameters, such as relative m/z fractions (measured by the AMS) showed a slight time trend. Therefore, the results shown in the next sections are given as average values of 30 to 90 min of nebulization (45 min for AMS; 90 min for H-TDMA and 30 min for TD-API-AMS), depending on the time step measurements of each instrument.

2.6 Reagents

10 Isoprene (Fluka 99.5%), α -pinene (Aldrich 98%), TMB (Fluka 99%), H_2O_2 (without stabilizer, Aldrich, 50 wt%), glyoxylic acid (Acros, 98%), pyruvic acid (Aldrich, 98%), oxalic acid (Sima-Aldrich, $\geq 99\%$), 3-butene-1,2-diol (Aldrich, $\geq 99\%$), D-erythrose (Sigma, $\geq 75\%$), DL-glyceraldehyde (ABCR, 40% in water), D-threitol (Aldrich, 99%), 2-methylfuran (Aldrich, 99%), 3-methylcrotonaldehyde (Aldrich, 97%), and methanol (Acros, HPLC grade) were used. Following the protocol described by Claeys et al. (2004b), 2,3-dihydroxymethacrylic acid (DHMA) was synthesized from methacrylic acid (Acros, 99.5%) by reaction with hydrogen peroxide (50% aqueous solution; 15 50 ml), in the presence of sulfuric acid (0.1 M; 25 ml). The pH of the mixture was around 2. The reaction mixture was shaken thoroughly and left at room temperature for 2 h before analysis. A detailed identification of this molecule by mass spectrometry can be found in Liu et al. (2009). The synthesis of 1-hydroxyethylhydroperoxide (1-HEHP) was performed by mixing pure acetaldehyde (6 μ l) and H_2O_2 (50% aqueous solution; 20 8 μ l) in 10 ml of pure water during five days prior to analysis. Solutions were prepared using UHQ water (Millipore), including reverse osmosis, micro-filtration, nuclear-grade deionization and activated carbon modules. The resistivity of the obtained water was greater than $1.8 \times 10^7 \Omega \text{ cm}^{-1}$. 25

Aqueous phase processing of secondary organic aerosols

Y. Liu et al.

Title Page

Abstract

Introduction

Conclusions

References

Tables

Figures

⏪

⏩

◀

▶

Back

Close

Full Screen / Esc

Printer-friendly Version

Interactive Discussion



3 Results and discussion

3.1 SOA formation in the smog chamber

Substantial quantities of SOA were formed in the smog chamber during the gas phase photooxidation of isoprene, α -pinene and TMB for all experiments (Fig. S1 in the Supplement). Maximum SOA concentrations were higher than $200 \mu\text{g m}^{-3}$. They were collected for 2 h at 6 l min^{-1} , and then extracted in 130 or 160 ml UHQ water (Millipore). The aqueous phase concentration of organic aerosol reached, after water extraction (and assuming a particle density of 1 g cm^{-3}), 0.4 mg l^{-1} for SOA generated from isoprene, and at least 0.9 mg l^{-1} for SOA generated from TMB and α -pinene. This organic concentration in the extract is similar to dissolved organic carbon (DOC) concentration found in bulk precipitation ($0.5\text{--}5 \text{ mg l}^{-1}$) at Zagreb and Sibenik, Croatia (Orlovic-Leko et al., 2009) and to the lower DOC concentration found in cloud water ($1\text{--}9 \text{ mg l}^{-1}$) at Puy de Dome, France (Marinoni et al., 2004). During the photooxidation of α -pinene and TMB, once nucleation had started, the particle size increased rapidly, and exceeded the measured range of the SMPS (i.e. $>685 \text{ nm}$) after 1:30 h and 3:30 h of photooxidation, respectively. This observation is due to the high initial concentrations of reactants introduced. Isoprene was introduced in even higher quantities (Table 1), but, due to its low ability to form SOA (Surratt et al., 2006; Dommen et al., 2009), the particles did not exceed the range of the SMPS (Fig. S1 in the Supplement). The number and size distribution showed a very good agreement between experiments 1 and 2 (Fig. S1a and b in the Supplement), during isoprene photooxidation performed under the same conditions. The total estimated masses of SOA collected on the filters were the same ($\pm 10\%$) for both experiments.

Aqueous phase processing of secondary organic aerosols

Y. Liu et al.

Title Page

Abstract

Introduction

Conclusions

References

Tables

Figures

⏪

⏩

◀

▶

Back

Close

Full Screen / Esc

Printer-friendly Version

Interactive Discussion



3.2 Influence of aqueous phase processing on SOA aging

3.2.1 AMS measurements

The bulk composition as measured by the AMS showed a slightly higher f_{44} (ratio of $m/z = 44$ to total organic aerosol) for the water extracted organic aerosol than from the direct chamber measurement. This is in very good agreement with the observations by Lee et al. (2011) who performed the same kind of SOA treatment and analysis, and is potentially due to the loss of less soluble species having a lower extraction efficiency than more oxidized species. The degree of oxidation can be characterized in terms of the two main ions $m/z = 44$ (CO_2^+) and $m/z = 43$ (mostly $\text{C}_2\text{H}_3\text{O}^+$), which were used to follow the aging of organic aerosol in the atmosphere by a compilation study of AMS data (Ng et al., 2010). In this study, low volatility oxygenated organic aerosol (LV-OOA) has a higher f_{44} component compared to the semi-volatile oxygenated organic aerosol (SV-OOA) which in turn has a higher f_{43} (ratio of $m/z = 43$ to total organic aerosol). Figure 2 compares the f_{44} versus f_{43} values to those provided in the compilation by Ng et al. (2010), and the results obtained by Lee et al. (2011). It is seen that the f_{44} versus f_{43} values obtained here fall close to the lower half of the triangular region defined by Ng et al. (2010). This region of the triangle is characteristic of lower O:C ratios and photochemical ages, and is the region where most of the laboratory SOA data are found (Ng et al., 2010; Lee et al., 2011). For the isoprene and α -pinene experiments No. 1 to 3, f_{43} decreases and f_{44} increases in “ $\text{H}_2\text{O}_2 + h\nu$ samples” compared to “control samples”. These observations show that aqueous phase photooxidation can induce SOA aging. Figure 2 shows that f_{44} values of our “ $\text{H}_2\text{O}_2 + h\nu$ sample” move towards the values of LV-OOA observed in the field by Ng et al. (2010). However, the aging effect observed here is small. This can be due to the difference of composition between laboratory generated and ambient SOA. In particular, the high initial precursor concentrations used here can induce the condensation of non polar organic compounds on SOA, which have a low water solubility. Finally, this can also be due to the low intensity of the xenon arc lamp used in the aqueous phase photoreactor. Although its spectrum

Aqueous phase processing of secondary organic aerosols

Y. Liu et al.

Title Page

Abstract

Introduction

Conclusions

References

Tables

Figures

⏪

⏩

◀

▶

Back

Close

Full Screen / Esc

Printer-friendly Version

Interactive Discussion



represented well that of the tropospheric sunlight in the UV-visible region, its intensity was only about 4 % of that of sunlight at noon in mid latitudes in summer. This observation can also explain that the aging effect obtained here was also small compared to the study by Lee et al. (2011) who used a Hg lamp, which spectrum is highly intense only at 254 nm, deeper in the UV region than the tropospheric sunlight.

3.2.2 H-TDMA measurements

For all nebulized samples, the H-TDMA data were taken into account during 90 min. The dependence of the hygroscopicity on particle composition can be represented with the hygroscopicity parameter κ . According to Petters and Kreidenweis (2007), the values of κ range from 0.01 to 0.5 for slightly to very hygroscopic organic species. The κ values obtained here for “control” samples are comprised between 0.04 and 0.08 for the three precursors, thus showing that the formed SOA are only slightly hygroscopic (Fig. 3). The hygroscopicity of the particles increases significantly from “control” samples ($\kappa = 0.04\text{--}0.08$) to “dark H_2O_2 ” samples ($\kappa = 0.06\text{--}0.10$) and to “ $\text{H}_2\text{O}_2 + h\nu$ ” samples ($\kappa = 0.1\text{--}0.13$) for isoprene and α -pinene (Fig. 3a and b). This increase of hygroscopicity indicates that the aged SOA (formed after aqueous phase processing) contains more hygroscopic products. This result is consistent with the AMS data which show a clear increase of the f_{44}/f_{43} ratio from “control samples” to “ $\text{H}_2\text{O}_2 + h\nu$ samples” for isoprene and α -pinene. These observations of the bulk aerosol hygroscopic properties provide evidence that aqueous phase photooxidation induces SOA aging. Comparing the two experiments performed with isoprene, Fig. 3a shows that, although both experiments start at the same values of κ (for both selected particle diameters), the aqueous phase aging effect is significantly more pronounced for experiment 1 than for experiment 2. This observation is in excellent agreement with the AMS results. Figure 2 shows that the f_{44}/f_{43} ratios are the same for “control samples” for both experiments, while for “dark H_2O_2 ” and “ $\text{H}_2\text{O}_2 + h\nu$ ” samples, these ratios are significantly higher for experiment 1 than for experiment 2. The reason for this more pronounced aging effect is difficult to explain since the two experiments have been performed under

Aqueous phase processing of secondary organic aerosols

Y. Liu et al.

Title Page

Abstract

Introduction

Conclusions

References

Tables

Figures



Back

Close

Full Screen / Esc

Printer-friendly Version

Interactive Discussion



for isoprene and by a factor of 4.0 for α -pinene (Fig. 4). These factors were determined by a linear regression of the intensity of the major masses (most intense peaks) between the measurements from the smog chamber and the measurements after nebulization of “control samples”. The high correlation between each pair of measurements provides good evidence that the relative intensities are quite similar for isoprene and α -pinene ($R^2 = 0.88$ and 0.70 respectively), indicating that the chemical composition of SOA did not change significantly due to sampling, extraction and nebulization for isoprene and α -pinene. However, no correlation was observed for TMB ($R^2 = 0.12$), which can indicate significant changes of chemical composition during nebulization for the SOA from this precursor.

Because of the low signal intensity obtained with the nebulized aerosol measurements, and because of the discrepancy of TMB mass spectra from the chamber and after nebulization, no further direct comparison between smog chamber SOA and processed SOA was performed for our experiments. Only the results obtained for the aqueous phase chemical composition before and after processing are presented in detail below.

3.4 Influence of aqueous phase processing on SOA aging on the basis of aqueous phase chemical characterization

In order to investigate the effects of aqueous phase processing on the chemical composition of the sampled SOA (through oxidation by H_2O_2 in the dark or oxidation by OH radicals), comparisons between the chemical composition of (i) “control” samples and “ $\text{H}_2\text{O}_2 + h\nu$ ” samples (Fig. 5); (ii) “control” sample and “dark H_2O_2 ” samples (Fig. S2 in the Supplement); (iii) “dark H_2O_2 ” samples and “ $\text{H}_2\text{O}_2 + h\nu$ ” sample (Fig. S3 in the Supplement) were performed. The mass spectra, obtained by direct infusion into the APCI-MS, showed significant differences in the negative mode for isoprene and α -pinene.

For α -pinene, the formation of significant new signal was observed, especially in the mass range 80–200 Da (Fig. 5b). A comparison of this mass spectrum with the one

Aqueous phase processing of secondary organic aerosols

Y. Liu et al.

Title Page

Abstract

Introduction

Conclusions

References

Tables

Figures

⏪

⏩

◀

▶

Back

Close

Full Screen / Esc

Printer-friendly Version

Interactive Discussion



presented in Fig. 4b, indicates that most of the formed ions correspond to compounds observed in the initial SOA formation in the smog chamber. It is thus likely that the corresponding reaction products are already present in the SOA collected from the smog chamber and their formation is enhanced within the aqueous phase (Tan et al., 2009, 2010; El Haddad et al., 2009; Carlton et al., 2009). The effects of H₂O₂ cannot be compared to those of OH radicals, because of the lack of “dark H₂O₂” samples during α -pinene experiments (Table 1).

For isoprene, many new compounds were formed during the aqueous phase processing, as seen by new ions signal appeared in two distinct mass ranges: 60–150 Da, and 150–300 Da (Fig. 5a). By comparing the “H₂O₂ + *h* ν ” samples with the “dark H₂O₂” samples and “control” samples (Figs. S2 and S3 in the Supplement), it becomes clear that the formation of these ions in these two mass ranges were caused by both OH radicals and H₂O₂.

- In the mass range 60–150 Da, most of the ion masses correspond to those observed in SOA formed from gas phase reactions (Fig. 4a). It is thus likely that the aqueous phase aging of SOA leads to further formation of the corresponding products. Further identification of eleven of these aqueous phase products (in the mass range 60–150 Da) provide evidence for this assumption (see Sect. 3.5).
- In the mass range 150–300 Da, most of the ions are new compared to the initial SOA composition. Their molecular masses are 2–4 times higher than that of isoprene, and the observed distribution is consistent with the development of an oligomer system that shows a highly regular pattern of mass differences of 14, 16, 18 and 28 Da. Therefore, we assume that the corresponding products have been formed by aqueous phase oligomerization processes.

3.5 Discussion on the isoprene results

In order to discuss the results mentioned above concerning isoprene, a detailed study of the chemical composition of aqueous samples was performed for experiments 1

Aqueous phase processing of secondary organic aerosols

Y. Liu et al.

Title Page

Abstract

Introduction

Conclusions

References

Tables

Figures



Back

Close

Full Screen / Esc

Printer-friendly Version

Interactive Discussion



and 2. The identification of reaction products was done in “H₂O₂ + hν” samples using APCI-MS² during experiment 1. Additionally, in order to determine the effects of aqueous phase processing on SOA composition, the abundance of 33 specific products was compared between “H₂O₂ + hν” samples, “dark H₂O₂” samples and “control” samples using HPLC-MS during experiment 2. The results obtained using these two complementary analyses are discussed in the following, for the mass ranges 60–150 Da and 150–300 Da separately.

3.5.1 Mass range 60–150 Da

Identification using APCI-MS²

During experiment 1, nine reaction products were identified in “H₂O₂ + hν” samples using APCI-MS² in the positive and in the negative modes. The identification was performed by comparison of the APCI-MS² fragments between “H₂O₂ + hν” samples and those of commercial or synthesized standards with exact or similar chemical structures (Table 2). We identified 2-methylbut-3-ene-1,2-diol (MB-diol), 2,3-dihydroxy-2-methylpropanal (DHMP), trihydroxy-3-methylbutanal (THMB), 2-methylbutane-1,2,3,4-tetrol (tetrol) in the negative mode using commercial standards that had the same chemical structure except for a methyl group. The obtained mass spectra were similar, with a systematic shift of 14 Da corresponding to the missing methyl group in the standards. We identified 3-methylfuran (3-MF) and 3-methylbut-3-enal (MB-3-enal) in the positive mode with commercial standard isomers. Finally, 1-hydroxyethyl-hydroperoxide (1-HEHP) and 2,3-dihydroxy-methacrylicacid (DHMA) were identified using synthesized standards (see reagents). All these identified reaction products fall in the mass range 60–150 Da, and have been identified in SOA formed from isoprene photooxidation in earlier studies (Surratt et al., 2006; Edney et al., 2005; Ion et al., 2005; Kourtchev et al., 2005). Furthermore, some of them (such as DHMA and tetrol) have also been observed as constituents of atmospheric SOA in rural and/or forested area (Kourtchev et al., 2005; Claeys et al., 2004a; Ion et al., 2005; Sullivan et al., 2007; Kawamura et

Aqueous phase processing of secondary organic aerosols

Y. Liu et al.

Title Page

Abstract

Introduction

Conclusions

References

Tables

Figures

⏪

⏩

◀

▶

Back

Close

Full Screen / Esc

Printer-friendly Version

Interactive Discussion



al., 1999) and water droplets in a power plant plume, in clean clouds as well as in a maritime area (Sorooshian et al., 2006b; Warneck 2003).

Quantification using HPLC-MS and IC-MS

During experiment 2, HPLC-MS and IC-MS measurements were performed for the liquid samples, in order to compare the quantity of the 16 identified compounds between “H₂O₂ + *hν*” samples, “dark H₂O₂” samples and “control” samples (Table 2). The HPLC-MS and IC-MS techniques allowed separating species that had the same molecular mass and for a quantitative comparison between the three samples, which is much more precise than the direct infusion method. Because no systematic calibration was performed for all these compounds, and because the analyses of the three samples were performed under the same conditions, the chromatographic peak areas (which are proportional to the aqueous phase concentrations under our experimental conditions) are compared in Table 2. All peak areas were normalized to “control sample”. The analytic standard deviation was 3 to 14 % for HPLC-MS analysis, and varied from 1 to 25 % for IC-MS analysis, depending on the species and their concentrations.

Among the 16 compounds, the concentrations of formic, glyoxylic, glycolic, butyric, oxalic acid, DHMA, THMB, MB-diol, MB-3-enal, increased significantly in the “H₂O₂ + *hν*” samples and “dark H₂O₂” samples compared to the “control” samples (Table 2). It is thus likely that these compounds are produced in the aqueous phase by oxidation of water soluble precursors by H₂O₂ and by photooxidation. The potential precursors are small multifunctional carbonyls (glycolaldehyde, hydroxyacetone, glyoxal, methylglyoxal, hydroxymethylglyoxal, oxopropanedial, 2,3-dioxobutanal) that have been specifically studied by Healy et al. (2008) on SOA formed from isoprene photooxidation in smog chambers under similar conditions as ours. All these precursors are highly water soluble, thus they were likely transferred to the aqueous phase in our experiments, and were then oxidized. The aqueous phase photooxidation of glycolaldehyde (studied by Perri et al., 2009) leads to the formation of glyoxal (which could not be detected with our instruments), but also to glycolic, glyoxylic and oxalic

Aqueous phase processing of secondary organic aerosols

Y. Liu et al.

Title Page

Abstract

Introduction

Conclusions

References

Tables

Figures

⏪

⏩

◀

▶

Back

Close

Full Screen / Esc

Printer-friendly Version

Interactive Discussion



**Aqueous phase
processing of
secondary organic
aerosols**

Y. Liu et al.

Title Page

Abstract

Introduction

Conclusions

References

Tables

Figures

⏪

⏩

◀

▶

Back

Close

Full Screen / Esc

Printer-friendly Version

Interactive Discussion

acid which concentrations increase from the “control” to the “ $\text{H}_2\text{O}_2 + h\nu$ ” samples in the present study (Table 2). The formation of glyoxylic and oxalic acids has also been observed during the aqueous phase photooxidation of methylglyoxal (by Altieri et al., 2008; Tan et al., 2010) and glyoxal (Carlton et al., 2007; Tan et al., 2009), which are among the potential precursors identified by Healy et al. (2008). The aqueous phase photooxidation of the other precursors has not yet been studied (to our knowledge), but they are likely to produce the acids that have been observed to increase in the present study from the “control” to the “ $\text{H}_2\text{O}_2 + h\nu$ ” samples. It can be noted that formic and oxalic acids show among the largest increase, which is in good agreement with the fact that these compounds are end chain reaction products and are stable towards most of reactants in the atmosphere, as it was shown by field observations (Yao et al., 2003; Legrand et al., 2005, 2007; Sorooshian et al., 2006b).

For pyruvic acid, DHMP and tetrol, a significant decrease of their concentrations is observed between the “control” sample and the “ $\text{H}_2\text{O}_2 + h\nu$ ” sample, and between the “control” samples and “dark H_2O_2 ” samples, thus showing that they were consumed by oxidation by H_2O_2 and photooxidation. This observation is in agreement with the studies by Guzmán et al. (2006), Carlton et al. (2006) and Altieri et al. (2006) who have shown that in the aqueous phase pyruvic acid is photosensitive and highly reactive towards OH radicals, leading to the formation of oxalic acid (among other products), which has been observed to increase from the “control” sample to the “ $\text{H}_2\text{O}_2 + h\nu$ ” sample in the present study.

The concentrations of 1-HEHP show a particular behaviour: they increase significantly in the “dark H_2O_2 ” sample and “ $\text{H}_2\text{O}_2 + h\nu$ ” sample compared to “control” sample, and they decrease significantly in “ $\text{H}_2\text{O}_2 + h\nu$ ” sample compared to “dark H_2O_2 ” sample. This behaviour can be explained by aqueous phase formation of this compound by the oxidation by H_2O_2 of larger compounds containing hydroxyl groups, and by further OH oxidation and/or direct photolysis of 1-HEHP (as it was shown by Monod et al., 2007).

The concentrations of 3-methylfuran do not show any significant changes between “control” sample, “dark H₂O₂” sample and “H₂O₂ + *hν*” sample. The reason for this behaviour may be that this compound was produced and consumed in the aqueous phase in roughly the same quantities.

5 Finally the concentrations of lactic acid and methylmaleic acid show a significant change between “dark H₂O₂” sample and the two other samples, but we do not have any explanation for this trend.

10 Overall, the effects of photooxidation were unexpectedly comparable to those of H₂O₂ (in the dark). This observation can be explained by (i) the amounts of H₂O₂ used (calculated using several hypotheses, see Sect. 2.4), and ii) the low intensity of the xenon lamp within the photoreactor (which corresponded only to roughly 4 % of the sun light at noon in mid latitudes during the summer).

15 Among the compounds that are produced in the aqueous phase, DHMA and THMB correspond to the oxidized forms of DHMP and tetrol respectively, which are consumed in the aqueous phase. It is thus probable that the aqueous phase oxidation of DHMP and tetrol by H₂O₂ and/or by OH radicals leads to DHMA and THMB respectively, following the chemical mechanisms proposed in Fig. 6a and b.

3.5.2 In the mass range 150–300 Da

20 As shown in Fig. 5a, the formation of many new ions was detected in the mass range 150–300 Da, with the development of an oligomer system which was due to aqueous phase processing (as described in Sect. 3.4). In this mass range, five ions were analyzed by HPLC-MS and APCI-MS². The HPLC-MS analysis showed that these five ions had different retention times (between 5.5 and 7 min for *m/z* = 169⁻, 171⁻, 153⁺ Da; 42 min for *m/z* = 183⁻ Da, and 64 min for *m/z* = 233⁻ Da), thus attributing them to different reaction products. These five compounds were characterized using APCI-MS²
25 fragmentation (Fig. 7). Neutral losses of 18, 28, 30 and 46 indicate that ion 153⁺ can be a hydroxyl-carbonyl compound, the neutral losses of 28, 30 and 44 indicate that

Aqueous phase processing of secondary organic aerosols

Y. Liu et al.

Title Page

Abstract

Introduction

Conclusions

References

Tables

Figures

⏪

⏩

◀

▶

Back

Close

Full Screen / Esc

Printer-friendly Version

Interactive Discussion



ions 169⁻, 183⁻ and 233⁻ can be oxo-carboxylic acids, and the neutral losses of 18 and 44 indicate that ion 171⁻ can be a hydroxy-carboxylic acid or a dicarboxylic acid.

Some of the potential precursors (glycolaldehyde, glyoxal, methylglyoxal) of the reaction products discussed in Sect. 3.5.1 have been shown to produce oligomers through aqueous phase photooxidation (Altieri et al., 2006, 2008; Carlton et al., 2006, 2007; Perri et al., 2009; El Haddad et al., 2009; Tan et al., 2009, 2010; Zhang et al., 2010; Liu et al., 2011). Despite the very good agreement of the present study with previous work concerning the formation of small polyfunctional compounds through aqueous phase photooxidation of these potential precursors (Sect. 3.5.1), the oligomer formation seems to behave very differently. Comparing the most intense peaks of the mass spectra obtained in the present study (above 150 Da) with those described in the literature, no concordance is achieved except for two ions:

- At 171 Da in the negative mode: the fragmentation spectrum obtained for this ion is very similar to the one obtained by El Haddad et al. (2009) (with the same instrument, operated under the same conditions) during the aqueous phase OH oxidation of methacrolein, at 20 h of reaction (Fig. 7). However, methacrolein (one of the major gas-phase reaction products of isoprene) is highly volatile, and was not observed in the SOA by Healy et al. (2008). It is thus likely that ion 171⁻ is a reaction product formed in the aqueous phase from the photooxidation of common non volatile products of methacrolein and isoprene.
- At 233 Da in the negative mode: this ion has been observed by Perri et al. (2009) and by Altieri et al. (2008), during the aqueous phase photooxidation of glycolaldehyde and methylglyoxal, respectively. It was attributed to an oligomeric series consisting of the addition of oxalic acid to *n* molecules of methylglyoxal (with *n* = 2 in the case of ion *m/z* = 233⁻). However, the fragmentation of 233⁻ in the present study (Fig. 7) does not reveal the presence of a subunit 72 (i.e. methylglyoxal). It is thus probable that ion 233⁻ does not correspond to the same oligomer as the one described by Altieri et al. (2008) and Perri et al. (2009).

Aqueous phase processing of secondary organic aerosols

Y. Liu et al.

Title Page

Abstract

Introduction

Conclusions

References

Tables

Figures



Back

Close

Full Screen / Esc

Printer-friendly Version

Interactive Discussion



**Aqueous phase
processing of
secondary organic
aerosols**

Y. Liu et al.

[Title Page](#)[Abstract](#)[Introduction](#)[Conclusions](#)[References](#)[Tables](#)[Figures](#)[⏪](#)[⏩](#)[◀](#)[▶](#)[Back](#)[Close](#)[Full Screen / Esc](#)[Printer-friendly Version](#)[Interactive Discussion](#)

These observations may indicate that the oligomerization process was very different in the present study compared to previous work. If we compare our results more globally with the literature, we can say that we have observed the formation of oligomers between 150 and 300 Da, with a regular pattern of mass differences of 14, 16, 18 and 28 Da, whereas the previous studies have obtained oligomers up to 400, 500 and even 1200 Da, with highly regular patterns of mass differences of 12, 14, 16, 18 and 28 Da and also (depending on the precursor) 70 Da (methacrolein or methylvinylketone) and 72 Da (methylglyoxal). These large differences of mass spectral patterns can be explained by the difference in the initial conditions. In the present work, we have investigated aqueous phase processing of a complex mixture containing a low initial concentration of dissolved organic carbon (DOC) of 0.4 mg l^{-1} (Sect. 3.1), whereas the previous studies have investigated aqueous phase photooxidation of a single oxygenated compound at elevated initial concentrations, ranging from 17 to 1800 mg l^{-1} , thus 40 to 4000 times more concentrated than in our study. Very recently, it has been shown that oligomer formation depends highly on the initial concentration of the single compound in the aqueous phase. During the photooxidation of glyoxal (Tan et al., 2009), methylglyoxal (Tan et al., 2010) or methylvinylketone (Liu et al., 2011), oligomers higher than 150 Da were observed for initial concentrations higher than 17, 72 and 140 mg l^{-1} , respectively. Furthermore, in all these studies the oligomers were secondary products. It is thus likely that oligomerization processes occur between the initial precursor and its first generation reaction products or their corresponding radicals (Guzmán et al., 2006; Altieri et al., 2006, 2008; El Haddad et al., 2009; Tan et al., 2009, 2010). These processes may explain why we obtained here different oligomers at much lower reactant concentrations (by a factor of 40 to 4000). Since our complex initial mixture is likely more representative to real atmospheric conditions, more research is needed in order to investigate in more detail the effects of the initial complex DOC composition and concentrations on the aqueous phase oligomerization processes, and their chemical mechanisms.

4 Conclusions

This paper reports experimental results on the aging of SOA by photooxidation in the aqueous phase. After sampling and water extraction of SOA formed in the smog chamber, the liquid phase concentration of organic matter was in the range of DOC concentrations found in bulk precipitation and in cloud water. Comparing the nebulized SOA before and after aqueous phase processing (by H₂O₂ oxidation, and photooxidation) it was shown that the particles were significantly more hygroscopic after aqueous phase processing (observed with a H-TDMA). It was also shown that the particles contained more carboxylic functions (observed with an AMS), in agreement with previous recent studies of aqueous phase photochemical aging of SOA generated from dark ozonolysis of d-limonene (Bateman et al., 2011), of α -pinene (Lee et al., 2011), and also aqueous phase photochemical aging of atmospheric aerosols and cloud water collected in a coniferous forest mountain site (Lee et al., 2011). It is thus strongly evidenced that aqueous phase reactivity induces a significant impact on SOA aging. Furthermore, it is likely that this impact is highly different depending on the precursor. For example, the oligomeric compounds in the processed SOA was enriched when generated from isoprene photooxidation, was not impacted when generated from α -pinene photooxidation, and was depleted when generated from d-limonene ozonolysis (Bateman et al., 2011). In particular, for isoprene experiments, the processed SOA showed different oligomers starting from much lower aqueous phase DOC concentrations (by a factor of 40 to 4000) compared to previous studies who explored the aqueous phase fate of individual precursors. Since our complex initial mixture is likely more representative to real atmospheric conditions, more research is needed in order to investigate in more detail the effects of the initial complex DOC composition and concentrations on the aqueous phase oligomerization processes, and their chemical mechanisms.

For isoprene experiments, IC-MS and HPLC-APCI-MS analyses of the liquid phase showed the formation of 16 aqueous phase non-oligomeric reaction products (carboxylic acids or multifunctional oxygenated species), in good agreement with previous

Aqueous phase processing of secondary organic aerosols

Y. Liu et al.

[Title Page](#)[Abstract](#)[Introduction](#)[Conclusions](#)[References](#)[Tables](#)[Figures](#)[⏪](#)[⏩](#)[◀](#)[▶](#)[Back](#)[Close](#)[Full Screen / Esc](#)[Printer-friendly Version](#)[Interactive Discussion](#)

**Aqueous phase
processing of
secondary organic
aerosols**

Y. Liu et al.

Title Page

Abstract

Introduction

Conclusions

References

Tables

Figures

⏪

⏩

◀

▶

Back

Close

Full Screen / Esc

Printer-friendly Version

Interactive Discussion

works that have explored the aqueous phase photooxidation of individual precursors. A chemical mechanism was proposed to explain the observation of aqueous phase consumption or formation of four of these compounds: aqueous phase oxidation of DHMP leading to DHMA; and aqueous phase oxidation of tetrol leading to THMB. The aqueous phase kinetic rate constant of tetrol towards OH radical is estimated to be $2.2 \times 10^9 \text{ l mol}^{-1} \text{ s}^{-1}$, (based on the SAR estimation method developed by Monod and Doussin, 2008). The corresponding aqueous phase lifetime is estimated to range from several minutes to several hours in the atmosphere. As tetrols are used as marker compounds of isoprene SOA (El Haddad et al., 2011), the degradation of tetrols by OH radicals in the aqueous phase might induce underestimations in the amount of biogenic SOA in the atmosphere.

Overall, the effects of H_2O_2 oxidation (in the dark) were unexpectedly comparable to those of photooxidation. This observation can be explained by the low intensity of the xenon lamp used in the photoreactor. The gas phase experiments were done under high NO_x conditions in the smog chamber, thus no hydroperoxides were formed. Because of the very low water solubility of NO_x , their chemistry cannot take place in the aqueous phase (Monod and Carlier, 1999). In this case, it facilitates the aqueous phase peroxidation of the soluble organic compounds, such as carbonyls that lead to the formation of peracids (Liu et al., 2009). Under natural conditions, H_2O_2 can be formed through aqueous phase reactivity (Möller, 2009, and references therein), thus, the addition of H_2O_2 (to form OH radicals by photolysis) was quite realistic in our approach. Nevertheless, to simulate more realistic atmospheric conditions, this kind of approach should be complemented by real multiphase studies where gas and aqueous phase reactions occur simultaneously. However, in this case, it is difficult to analyse each phase separately, thus our approach is the only one that allows one to investigate thoroughly each phase. For example, we could show here (using a TD-API-AMS) that sampling, extraction and/or nebulization did not significantly impact the chemical composition of SOA formed from isoprene and α -pinene, whereas it affected those formed from TMB. Further studies are needed to investigate which step impacted the

SOA formed from TMB. Still this example emphasizes that it is worthwhile to associate the two kinds of approaches complementarily.

Supplementary material related to this article is available online at:

<http://www.atmos-chem-phys-discuss.net/11/21489/2011/>

[acpd-11-21489-2011-supplement.pdf](#).

Acknowledgements. This study was funded by INTROP (ESF), EUROCHAMP, Réseau ERICHE and the Provence-Alpes-Côte-d'Azur Region, INSU-LEFE-CHAT, the ANR-blanc (project CUMULUS), as well as the Swiss National Science Foundation. The authors thank Rafal Strekowski for his help for the instruments shipping from the University of Provence to the Paul Scherrer Institute.

References

Altieri, K. E., Carlton, A. G., Lim, H. J., Turpin, B. J., and Seitzinger, S. P.: Evidence for oligomer formation in clouds: reactions of isoprene oxidation products, *Environ. Sci. Technol.*, 40, 4956–4960, 2006.

Altieri, K. E., Seitzinger, S. P., Carlton, A. G., Turpin, B. J., Klein, G. C., and Marshall, A. G.: Oligomers formed through in-cloud methylglyoxal reactions: Chemical composition, properties, and mechanisms investigated by ultra-high resolution FT-ICR mass spectrometry, *Atmos. Environ.*, 42, 1476–1490, 2008.

Baltensperger, U., Kalberer, M., Dommen, J., Paulsen, D., Alfarra, M. R., Coe, H., Fisseha, R., Gascho, A., Gysel, M., Nyeki, S., Sax, M., Steinbacher, M., Prévôt, A. S. H., Sjögren, S., Weingartner, E., and Zenobi, R.: Secondary organic aerosols from anthropogenic and biogenic precursors, *Faraday Discuss.*, 130, 265–278, 2005.

Bateman, A. P., Nizkorodov, S. A., Laskinb, J., and Laskinc, A.: Photolytic processing of secondary organic aerosols dissolved in cloud droplets, *Phys. Chem. Chem. Phys.*, 13, 12199–12212, 2011.

ACPD

11, 21489–21532, 2011

Aqueous phase processing of secondary organic aerosols

Y. Liu et al.

Title Page

Abstract

Introduction

Conclusions

References

Tables

Figures

◀

▶

◀

▶

Back

Close

Full Screen / Esc

Printer-friendly Version

Interactive Discussion



**Aqueous phase
processing of
secondary organic
aerosols**

Y. Liu et al.

Title Page

Abstract

Introduction

Conclusions

References

Tables

Figures

⏪

⏩

◀

▶

Back

Close

Full Screen / Esc

Printer-friendly Version

Interactive Discussion



- Camredon, M., Hamilton, J. F., Alam, M. S., Wyche, K. P., Carr, T., White, I. R., Monks, P. S., Rickard, A. R., and Bloss, W. J.: Distribution of gaseous and particulate organic composition during dark α -pinene ozonolysis, *Atmos. Chem. Phys.*, 10, 2893–2917, doi:10.5194/acp-10-2893-2010, 2010.
- 5 Carlton, A. G., Turpin, B. J., Lim, H., Altieri, K. E., and Seitzinger, S.: Link between isoprene and secondary organic aerosol (SOA): pyruvic acid oxidation yields low volatility organic acids in clouds, *Geophys. Res. Lett.*, 33, L06822/1–L06822/4, doi:10.1029/2005GL025374, 2006.
- Carlton, A. G., Turpin, B. J., Altieri, K. E., Seitzinger, S., Reff, A., Lim, H. J., and Ervens, B.: Atmospheric oxalic acid and SOA production from glyoxal: results of aqueous photooxidation experiments, *Atmos. Environ.*, 41, 7588–7602, 2007.
- 10 Carlton, A. G., Wiedinmyer, C., and Kroll, J. H.: A review of Secondary Organic Aerosol (SOA) formation from isoprene, *Atmos. Chem. Phys.*, 9, 4987–5005, doi:10.5194/acp-9-4987-2009, 2009.
- Claeys, M., Graham, B., Vas, G., Wang, W., Vermeylen, R., Pashynska, V., Cafmeyer, J., Guyon, P., Andreae, M. O., Artaxo, P., and Maenhaut, W.: Formation of secondary organic aerosols through photooxidation of isoprene, *Science*, 303, 1173–1176, 2004a.
- Claeys, M., Wang, W., Ion, A. C., Kourtchev, I., Gelencser, A., and Maenhaut, W.: Formation of secondary organic aerosols from isoprene and its gas-phase oxidation products through reaction with hydrogen peroxide, *Atmos. Environ.*, 38, 4093–4098, 2004b.
- 20 DeCarlo, P. F., Kimmel, J. R., Trimborn, A., and Northway, M. J.: Field-deployable, high-resolution, time-of-flight aerosol mass spectrometer, *Anal. Chem.*, 78, 8281–8289, 2006.
- Dommen, J., Metzger, A., Duplissy, J., Kalberer, M., Alfarra, M. R., Gascho, A., Weingartner, E., Prevot, A. S. H., Verheggen, B., and Baltensperger, U.: Laboratory observation of oligomers in the aerosol from isoprene/ NO_x photooxidation, *Geophys. Res. Lett.*, 33, L13805/1–L13805/5, 2006.
- 25 Dommen, J., Hellen, H., Saurer, M., Jäggi, M., Siegwolf, R., Metzger, A., Duplissy, J., Fierz, M., and Baltensperger, U.: Determination of the aerosol yield of isoprene in the presence of an organic seed with carbon isotope analysis, *Environ. Sci. Technol.*, 43, 6697–6702, 2009.
- Edney, E. O., Kleindienst, T. E., Jaoui, M., Lewandowski, M., Offenberg, J. H., Wang, W., and Claeys, M.: Formation of 2-methyl tetrols and 2-methylglyceric acid in secondary organic aerosol from laboratory irradiated isoprene/ NO_x / SO_2 /air mixtures and their detection in ambient $\text{PM}_{2.5}$ samples collected in the eastern United States, *Atmos. Environ.*, 39, 5281–5289, 2005.

**Aqueous phase
processing of
secondary organic
aerosols**

Y. Liu et al.

[Title Page](#)[Abstract](#)[Introduction](#)[Conclusions](#)[References](#)[Tables](#)[Figures](#)[⏪](#)[⏩](#)[◀](#)[▶](#)[Back](#)[Close](#)[Full Screen / Esc](#)[Printer-friendly Version](#)[Interactive Discussion](#)

- El Haddad, I., Yao Liu, Nieto-Gligorovski, L., Michaud, V., Temime-Roussel, B., Quivet, E., Marchand, N., Sellegri, K., and Monod, A.: In-cloud processes of methacrolein under simulated conditions - Part 2: Formation of secondary organic aerosol, *Atmos. Chem. Phys.*, 9, 5107–5117, doi:10.5194/acp-9-5107-2009, 2009.
- 5 El Haddad, I., Marchand, N., Temime-Roussel, B., Wortham, H., Piot, C., Besombes, J.-L., Baduel, C., Voisin, D., Armengaud, A., and Jaffrezo, J.-L.: Insights into the secondary fraction of the organic aerosol in a Mediterranean urban area: Marseille, *Atmos. Chem. Phys.*, 11, 2059–2079, doi:10.5194/acp-11-2059-2011, 2011.
- Eyglunent, G., Le Person, A., Dron, J., Monod, A., Voisin, D., Mellouki, A., Marchand, N., and Wortham, H.: Simple and reversible transformation of an APCI/MS/MS into an aerosol mass spectrometer: development and characterization of a new inlet, *Aerosol Sci. Tech.*, 42, 182–193, doi:10.1080/02786820801922946, 2008.
- Guzmán, M. I., Colussi, A. I., and Hoffmann, M. R.: Photoinduced oligomerization of aqueous pyruvic acid, *J. Phys. Chem. A*, 110, 3619–3626, 2006.
- 15 Gysel, M., McFiggans, G. B., and Coe, H.: Inversion of tandem differential mobility analyser (TDMA) measurements, *J. Aerosol Sci.*, 40, 134–151, doi:10.1016/j.jaerosci.2008.07.013, 2009.
- Hallquist, M., Wenger, J. C., Baltensperger, U., Rudich, Y., Simpson, D., Claeys, M., Dommen, J., Donahue, N. M., George, C., Goldstein, A. H., Hamilton, J. F., Herrmann, H., Hoffmann, T., Iinuma, Y., Jang, M., Jenkin, M. E., Jimenez, J. L., Kiendler-Scharr, A., Maenhaut, W., McFiggans, G., Mentel, Th. F., Monod, A., Prévôt, A. S. H., Seinfeld, J. H., Surratt, J. D., Szmigielski, R., and Wildt, J.: The formation, properties and impact of secondary organic aerosol: current and emerging issues, *Atmos. Chem. Phys.*, 9, 5155–5236, doi:10.5194/acp-9-5155-2009, 2009.
- 20 Healy, R. M., Wenger, J. C., Metzger, A., Duplissy, J., Kalberer, M., and Dommen, J.: Gas/particle partitioning of carbonyls in the photooxidation of isoprene and 1,3,5-trimethylbenzene, *Atmos. Chem. Phys.*, 8, 3215–3230, doi:10.5194/acp-8-3215-2008, 2008.
- Hellen, H., Dommen, J., Metzger, A., Gascho, A., Duplissy, J., Tritscher, T., Prévôt, A. S. H., and Baltensperger, U.: Using proton transfer reaction mass spectrometry for online analysis of secondary organic aerosols, *Environ. Sci. Technol.*, 42, 7347–7353, 2008.
- 30 Hua, W., Chen, Z. M., Jie, C. Y., Kondo, Y., Hofzumahaus, A., Takegawa, N., Chang, C. C., Lu, K. D., Miyazaki, Y., Kita, K., Wang, H. L., Zhang, Y. H., and Hu, M.: Atmospheric hydrogen peroxide and organic hydroperoxides during PRIDE-PRD'06, China: their concentration,

formation mechanism and contribution to secondary aerosols, *Atmos. Chem. Phys.*, 8, 6755–6773, doi:10.5194/acp-8-6755-2008, 2008.

linuma, Y., Böge, O., Gnauk, T., and Herrmann, H.: Aerosol-chamber study of the α -pinene/O₃ reaction: influence of particle acidity on aerosol yields and products, *Atmos. Environ.*, 38, 761–773, 2004.

Ion, A. C., Vermeylen, R., Kourtchev, I., Cafmeyer, J., Chi, X., Gelencsér, A., Maenhaut, W., and Claeys, M.: Polar organic compounds in rural PM_{2.5} aerosols from K-pusztá, Hungary, during a 2003 summer field campaign: Sources and diel variations, *Atmos. Chem. Phys.*, 5, 1805–1814, doi:10.5194/acp-5-1805-2005, 2005.

Jimenez, J. L., Canagaratna, M. R., Donahue, N. M., Prevot, A. S., Zhang, Q., Kroll, J. H., DeCarlo, P. F., Allan, J. D., Coe, H., Ng, N. L., Aiken, A. C., Docherty, K. S., Ulbrich, I. M., Grieshop, A. P., Robinson, A. L., Duplissy, J., Smith, J. D., Wilson, K. R., Lanz, V. A., Hueglin, C., Sun, Y. L., Tian, J., Laaksonen, A., Raatikainen, T., Rautiainen, J., Vaattovaara, P., Ehni, M., Kulmala, M., Tomlinson, J. M., Collins, D. R., Cubison, M. J., Dunlea, E. J., Huffman, J. A., Onasch, T. B., Alfarra, M. R., Williams, P. I., Bower, K., Kondo, Y., Schneider, J., Drewnick, F., Borrmann, S., Weimer, S., Demerjian, K., Salcedo, D., Cottrell, L., Griffin, R., Takami, A., Miyoshi, T., Hatakeyama, S., Shimojo, A., Sun, J. Y., Zhang, Y. M., Dzepina, K., Kimmel, J. R., Sueper, D., Jayne, J. T., Herndon, S. C., Trimborn, A. M., Williams, L. R., Wood, E. C., Middlebrook, A. M., Kolb, C. E., Baltensperger, U., and Worsnop, D. R.: Evolution of organic aerosols in the atmosphere, *Science*, 326, 1525–1529, doi:10.1126/science.1180353, 2009.

Kalberer, M., Paulsen, D., Sax, M., Steinbacher, M., Dommen, J., Prevot, A. S. H., Fisseha, R., Weingartner, E., Frankevich, V., Zenobi, R., and Baltensperger, U.: Identification of polymers as major components of atmospheric organic aerosols, *Science*, 303, 1659–1662, 2004.

Kawamura, K. and Sakaguchi, F.: Molecular distributions of water soluble dicarboxylic acids in marine aerosols over the Pacific Ocean including tropics, *J. Geophys. Res.*, 104(D3), 3501–3509, 1999.

Kawamura, K., Steinberg, S., Ng, L., and Kaplan, I. R.: Wet deposition of low molecular weight mono- and di-carboxylic acids, aldehydes and inorganic species in Los Angeles, *Atmos. Environ.*, 35, 3917–3926, 2001.

Kourtchev, I., Ruuskanen, T., Maenhaut, W., Kulmala, M., and Claeys, M.: Observation of 2-methyltetrols and related photo-oxidation products of isoprene in boreal forest aerosols from Hyytiälä, Finland, *Atmos. Chem. Phys.*, 5, 2761–2770, doi:10.5194/acp-5-2761-2005, 2005.

Aqueous phase processing of secondary organic aerosols

Y. Liu et al.

Title Page

Abstract

Introduction

Conclusions

References

Tables

Figures

◀

▶

◀

▶

Back

Close

Full Screen / Esc

Printer-friendly Version

Interactive Discussion

**Aqueous phase
processing of
secondary organic
aerosols**Y. Liu et al.

[Title Page](#)[Abstract](#)[Introduction](#)[Conclusions](#)[References](#)[Tables](#)[Figures](#)[⏪](#)[⏩](#)[◀](#)[▶](#)[Back](#)[Close](#)[Full Screen / Esc](#)[Printer-friendly Version](#)[Interactive Discussion](#)

- Kroll, J. H. and Seinfeld, J. H.: Chemistry of secondary organic aerosol: Formation and evolution of low-volatility organics in the atmosphere, *Atmos. Environ.*, 42, 3593–3624, 2008.
- Lanz, V. A., Alfarra, M. R., Baltensperger, U., Buchmann, B., Hueglin, C., and Prévôt, A. S. H.: Source apportionment of submicron organic aerosols at an urban site by factor analytical modelling of aerosol mass spectra, *Atmos. Chem. Phys.*, 7, 1503–1522, doi:10.5194/acp-7-1503-2007, 2007.
- Lee, A. K. Y., Herckes, P., Leaitch, W. R., Macdonald, A. M., and Abbatt, J. P. D.: Aqueous OH oxidation of ambient organic aerosol and cloud water organics: Formation of highly oxidized products, *Geophys. Res. Lett.*, 38, L11805, doi:10.1029/2011gl047439, 2011.
- 10 Legrand, M. and Puxbaum, H.: Summary of the CARBOSOL project: Present and retrospective state of organic versus inorganic aerosol over Europe, *J. Geophys. Res.*, 112, D23S01, doi:10.1029/2006JD008271, 2007.
- Legrand, M., Preunkert, S., Galy-Lacaux, C., Liousse, C., and Wagenbach, D.: Atmospheric year-round records of dicarboxylic acids and sulfate at three French sites located between 15 630 and 4360 m elevation, *J. Geophys. Res.*, 110, D13302, doi:10.1029/2004JD005515, 2005.
- Liu, Y., El Haddad, I., Scarfogliero, M., Nieto-Gligorovski, L., Temime-Roussel, B., Quivet, E., Marchand, N., Picquet-Varrault, B., and Monod, A.: In-cloud processes of methacrolein under simulated conditions - Part 1: Aqueous phase photooxidation, *Atmos. Chem. Phys.*, 9, 5093–5105, doi:10.5194/acp-9-5093-2009, 2009.
- 20 Liu, Y., Manoukian, A., Temime-Roussel, B., Voisin, D., and Monod, A.: Aqueous phase photooxidation of methyl vinyl ketone under simulated deliquescent aerosol conditions, in preparation, 2011.
- Marinoni, A., Laj, P., Sellegri, K., and Mailhot, G.: Cloud chemistry at the Puy de Dôme: variability and relationships with environmental factors, *Atmos. Chem. Phys.*, 4, 715–728, doi:10.5194/acp-4-715-2004, 2004.
- 25 Möller, D.: Atmospheric hydrogen peroxide: Evidence for aqueous-phase formation from a historic perspective and a one-year measurement campaign, *Atmos. Environ.*, 43, 5923–5936, 2009.
- 30 Monod, A. and Carlier P.: Impact of clouds on the tropospheric ozone budget: direct effect of multiphase photochemistry of soluble organic compounds, *Atmos. Environ.*, 33, 4431–4446, 1999.

**Aqueous phase
processing of
secondary organic
aerosols**

Y. Liu et al.

Title Page

Abstract

Introduction

Conclusions

References

Tables

Figures

⏪

⏩

◀

▶

Back

Close

Full Screen / Esc

Printer-friendly Version

Interactive Discussion

- Monod, A. and Doussin, J. F.: Structure-activity relationship for the estimation of OH-oxidation rate constants of aliphatic organic compounds in the aqueous phase: alkanes, alcohols, organic acids and bases, *Atmos. Environ.*, 42, 7611–7622, 2008.
- Monod, A., Chebbi, A., Durand-Jolibois, R., and Carlier, P.: Oxidation of methanol by hydroxyl radicals in aqueous solution under simulated cloud droplet conditions, *Atmos. Environ.*, 34, 5283–5294, 2000.
- Monod, A., Poulain, L., Grubert, S., Voisin, D., and Wortham, H.: Kinetics of OH-initiated oxidation of oxygenated organic compounds in the aqueous phase: new rate constants, structure-activity relationships and atmospheric implications, *Atmos. Environ.*, 39, 7667–7688, 2005.
- Monod, A., Chevallier, E., Durand-Jolibois, R., Doussin, J. F., Picquet-Varrault, B., and Carlier, P.: Photooxidation of methylhydroperoxide and ethylhydroperoxide in the aqueous phase under simulated cloud droplet conditions, *Atmos. Environ.*, 41, 2412–2426, 2007.
- Müller, L., Reinnig, M.-C., Warnke, J., and Hoffmann, Th.: Unambiguous identification of esters as oligomers in secondary organic aerosol formed from cyclohexene and cyclohexene/ α -pinene ozonolysis, *Atmos. Chem. Phys.*, 8, 1423–1433, doi:10.5194/acp-8-1423-2008, 2008.
- Ng, N. L., Canagaratna, M. R., Zhang, Q., Jimenez, J. L., Tian, J., Ulbrich, I. M., Kroll, J. H., Docherty, K. S., Chhabra, P. S., Bahreini, R., Murphy, S. M., Seinfeld, J. H., Hildebrandt, L., Donahue, N. M., DeCarlo, P. F., Lanz, V. A., Prévôt, A. S. H., Dinar, E., Rudich, Y., and Worsnop, D. R.: Organic aerosol components observed in Northern Hemispheric datasets from Aerosol Mass Spectrometry, *Atmos. Chem. Phys.*, 10, 4625–4641, doi:10.5194/acp-10-4625-2010, 2010.
- Offenberg, J. H., Jaoui, M., Kleindienst, T. E., Lewandowski, M., Lewis, C. W., and Edney, E. O.: Contribution of toluene and α -pinene to SOA formed in an irradiated α -pinene/toluene/ NO_x air mixture: comparison of results using ^{14}C content and SOA organic tracer methods, *Environ. Sci. Technol.*, 41, 3972–3976, 2007.
- Orlovic-Leko, P., Plavsic, M., Bura-Nakic, E., Kozarac, Z., and Cosovic, B.: Organic matter in the bulk precipitations in Zagreb and Sibenik, Croatia, *Atmos. Environ.*, 43, 805–811, 2009.
- Paulsen, D., Dommen, J., Kalberer, M., Prévôt, A. S. H., Richter, R., Sax, M., Steinbacher, M., Weingartner, E., and Baltensperger, U.: Secondary organic aerosol formation by irradiation of 1,3,5-trimethylbenzene- NO_x - H_2O in a new reaction chamber for atmospheric chemistry and physics, *Environ. Sci. Technol.*, 39, 2668–2678, 2005.

**Aqueous phase
processing of
secondary organic
aerosols**

Y. Liu et al.

Title Page

Abstract

Introduction

Conclusions

References

Tables

Figures

⏪

⏩

◀

▶

Back

Close

Full Screen / Esc

Printer-friendly Version

Interactive Discussion



Paulsen, D., Weingartner, E., Alfarra, M. R., and Baltensperger, U.: Volatility measurements of photochemically and nebulizer generated organic aerosol particles, *J. Aerosol Sci.*, 37, 1025–1051, 2006.

Petters, M. D. and Kreidenweis, S. M.: A single parameter representation of hygroscopic growth and cloud condensation nucleus activity, *Atmos. Chem. Phys.*, 7, 1961–1971, doi:10.5194/acp-7-1961-2007, 2007.

Perri, M. J., Seitzinger, S. P., and Turpin, B. J.: Secondary organic aerosol production from aqueous photooxidation of glycolaldehyde: laboratory experiments, *Atmos. Environ.*, 43, 1487–1497, 2009.

Poulain, L., Katrib, Y., Isikli, E., Liu, Y., Wortham, H., Mirabel, P., Calvé, L. S., and Monod, A.: In-cloud multiphase behaviour of acetone in the troposphere: Gas uptake, Henry's law equilibrium and aqueous phase photooxidation, *Chemosphere*, 81, 312–320, 2010.

Rudich, Y., Donahue, M. N., and Mentel, F. T.: Aging of organic aerosol: bridging the gap between laboratory and field studies, *Ann. Rev. Chem.*, 58, 321–352, 2007.

Sorooshian, A., Lu, M.-L., Brechtel, F. J., Jonsson, H., Feingold, G., Flagan, R. C., and Seinfeld, J. H.: On the source of organic acid aerosol layers above clouds, *Environ. Sci. Technol.*, 41, 4647–4654, 2007a.

Sorooshian, A., Ng, N. L., Chan, A. W. H., Feingold, G., Flagan, R. C., and Seinfeld, J. H.: Particulate organic acids and overall water-soluble aerosol composition measurements from the 2006 Gulf of Mexico Atmospheric Composition and Climate Study (GoMACCS), *J. Geophys. Res.*, 112, D13201, doi:10.1029/2007JD008537, 2007b.

Sorooshian, A., Varutbangkul, V., Brechtel, F. J., Ervens, B., Feingold, G., Bahreini, R., Murphy, S. M., Holloway, J. S., Atlas, E. L., Buzorius, G., Jonsson, H., Flagan, R. C., and Seinfeld, J. H.: Oxalic acid in clear and cloudy atmospheres: Analysis of data from the International Consortium for Atmospheric Research on Transport and Transformation 2004, *J. Geophys. Res.*, 111, D23S45, doi:10.1029/2005JD006880, 2007b.

Sullivan, R. C. and Prather, K. A.: Investigations of the diurnal cycle and mixing state of oxalic acid in individual particles in Asian aerosol outflow, *Environ. Sci. Technol.*, 41, 8062–8069, 2007.

Sun, Y. L., Zhang, Q., Anastasio, C., and Sun, J.: Insights into secondary organic aerosol formed via aqueous-phase reactions of phenolic compounds based on high resolution mass spectrometry, *Atmos. Chem. Phys.*, 10, 4809–4822, doi:10.5194/acp-10-4809-2010, 2010.

**Aqueous phase
processing of
secondary organic
aerosols**

Y. Liu et al.

Title Page

Abstract

Introduction

Conclusions

References

Tables

Figures

⏪

⏩

◀

▶

Back

Close

Full Screen / Esc

Printer-friendly Version

Interactive Discussion



Surratt, J. D., Murphy, S. M., Kroll, J. H., Ng, N. L., Hildebrandt, L., Sorooshian, A., Szmigielski, R., Vermeylen, R., Maenhaut, W., Claeys, M., Flagan, R. C., and Seinfeld, J. H.: Chemical composition of secondary organic aerosol formed from the photooxidation of isoprene, *J. Phys. Chem. A*, 110, 9665–9690, 2006.

5 Tan, Y., Perri, M. J., Seitzinger, S. P., and Turpin, B. J.: Effects of precursor concentration and acidic sulfate in aqueous glyoxal-oh radical oxidation and implications for secondary organic aerosol, *Environ. Sci. Technol.*, 43, 8105–8112, 2009.

Tan, Y., Carlton, G. A., Seitzinger, S. P., and Turpin, B. J.: SOA from methylglyoxal in clouds and wet aerosols: measurement and prediction of key products, *Atmos. Environ.*, 44, 5218–5226, 10 2010.

Tolocka, M. P., Jang, M., Ginter, J. M., Cox, F. J., Kamens, R. M., and Johnston, M. V.: Formation of oligomers in secondary organic aerosol, *Environ. Sci. Technol.*, 38, 1428–1434, 2004.

15 Tritscher, T., Dommen, J., DeCarlo, P. F., Barmet, P. B., Praplan, A. P., Weingartner, E., Gysel, M., Prévôt, A. S. H., Riipinen, I., Donahue, N. M., and Baltensperger, U.: Volatility and hygroscopicity of aging secondary organic aerosol in a smog chamber, *Atmos. Chem. Phys. Discuss.*, 11, 7423–7467, doi:10.5194/acpd-11-7423-2011, 2011.

van Pinxteren, D., Plewka, A., Hofmann, D., Mueller, K., Kramberger, H., Srvcina, B., Baechmann, K., Jaeschke, W., Mertes, S., Collett, J. L., and Herrmann, H.: Schmucke hill cap cloud and valley stations aerosol characterisation during FEBUKO (II): Organic compounds, 20 *Atmos. Environ.*, 39, 4305–4320, 2005.

Warneck, P.: In-cloud chemistry opens pathway to the formation of oxalic acid in the marine atmosphere, *Atmos. Environ.*, 37, 2423–2427, 2003.

25 Yao, X., Lau, A. P. S., Fang, M., Chan, C. K., and Hu, M.: Size distributions and formation of ionic species in atmospheric particulate pollutants in Beijing, China: 2. dicarboxylic acids, *Atmos. Environ.*, 37, 3001–3007, 2003.

Zhang, Q., Alfara, M. R., Worsnop, D. R., Allan, J. D., Coe, H., Canagaratna, M. R., and Jimenez, J. L.: Deconvolution and Quantification of Primary and Oxygenated Organic Aerosols Based on Aerosol Mass Spectrometry. Part 1: Development and Validation of the Method, *Environ. Sci. Technol.*, 39, 4938–4952, doi:4910.1021/es0485681, 2005.

30 Zhang, X., Chen, Z. M., and Zhao, Y.: Laboratory simulation for the aqueous OH-oxidation of methyl vinyl ketone and methacrolein: significance to the in-cloud SOA production, *Atmos. Chem. Phys.*, 10, 9551–9561, doi:10.5194/acp-10-9551-2010, 2010.

Aqueous phase processing of secondary organic aerosols

Y. Liu et al.

Title Page

Abstract

Introduction

Conclusions

References

Tables

Figures



Back

Close

Full Screen / Esc

Printer-friendly Version

Interactive Discussion



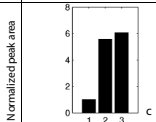
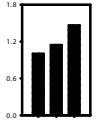
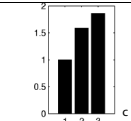
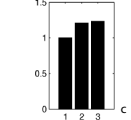
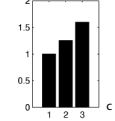
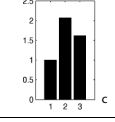
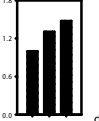
Table 1. Experimental conditions for smog chamber and aqueous phase experiments.

| Experiment number | Precursor | Smog chamber | | | | Aqueous phase photoreactor | | | | | |
|-------------------|--------------------------------------|--|---------------------------------|-----------------------|---------------------|--|---|--------------------------------------|-----|-------|-------------------|
| | | Initial concentration | | RH (%) and temp. (°C) | Particle collection | | Sample volume (ml) | | | | Reaction time (h) |
| VOC (ppm V) | NO _x ^a (ppm V) | Filters sampling time (hh:mm) ^b | Extraction volume of water (ml) | | "control" sample | "Dark H ₂ O ₂ " sample | "H ₂ O ₂ + hν" sample | [H ₂ O ₂] (M) | | | |
| 1 | Isoprene | 5.0 | 2.5 | 50–60% 20–25 °C | 03:40–05:40 | 160 | 30 | 30 | 100 | 0.1 | 20 |
| 2 | | 5.0 | 2.5 | | 02:50–04:50 | 160 | 30 | 30 | 100 | 0.1 | |
| 3 | <i>α</i> -pinene | 0.5 | 0.25 | | 02:40–04:40 | 130 | 30 | – | 100 | 0.015 | |
| 4 | TMB | 1.5 | 0.75 | | 03:40–05:40 | 160 | 30 | 30 | 100 | 0.045 | |

^a NO and NO₂ were injected in the same quantities for all experiments.

^b Time after lights were switched on in the smog chamber.

Table 2. Identification and quantification of reaction products during isoprene experiment 3, in the mass range 60-120 amu.

| Reaction product (molecular mass in g.mol ⁻¹) | Standards used for identification (molecular mass in g.mol ⁻¹) | Quantification |
|--|--|--|
| HCOOH (46) Formic acid | id ^a |  |
|  (74) Glyoxylic acid | id ^a |  |
|  (76) Glycolic acid | id ^a |  |
|  (88) Butyric acid | id ^a |  |
|  (90) Oxalic acid | id ^a |  |
|  (DHMA) (120) 2,3-dihydroxy-methacrylic acid | id ^b |  |
|  (THMB) (134) Trihydroxy-3-methylbutanal |  D-erythrose (120) ^a |  |

21523

**Aqueous phase
processing of
secondary organic
aerosols**

Y. Liu et al.

Title Page

Abstract

Introduction

Conclusions

References

Tables

Figures



Back

Close

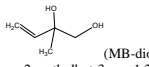
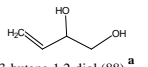
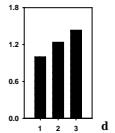
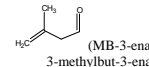
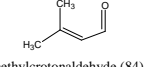
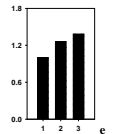
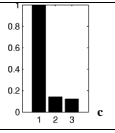
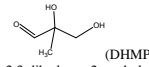
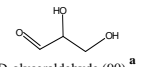
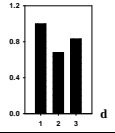
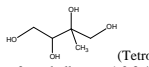
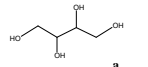
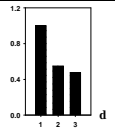
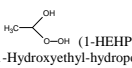
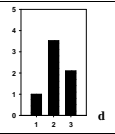
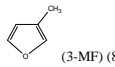
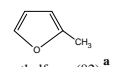
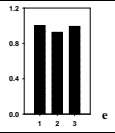
Full Screen / Esc

Printer-friendly Version

Interactive Discussion



Table 2. Continued.

| | | |
|---|---|---|
|  <p>(MB-diol) (102) 2-methylbut-3-ene-1,2-diol</p> |  <p>3-butene-1,2-diol (88) ^a</p> |  <p>d</p> |
|  <p>(MB-3-enal) (84) 3-methylbut-3-enal</p> |  <p>3-methylcrotonaldehyde (84) ^a</p> |  <p>e</p> |
|  <p>Pyruvic acid (88)</p> | <p>id ^a</p> |  <p>c</p> |
|  <p>(DHMP) (104) 2,3-dihydroxy-2-methyl-propanal</p> |  <p>D-glyceraldehyde (90) ^a</p> |  <p>d</p> |
|  <p>(Tetrol) (136) 2-methylbutane-1,2,3,4-tetrol</p> |  <p>D-Threitol (122) ^a</p> |  <p>d</p> |
|  <p>1-Hydroxyethyl-hydroperoxide (1-HEHP) (78)</p> | <p>id ^b</p> |  <p>d</p> |
|  <p>(3-MF) (82) 3-methylfuran</p> |  <p>2-methylfuran (82) ^a</p> |  <p>e</p> |

Aqueous phase processing of secondary organic aerosols

Y. Liu et al.

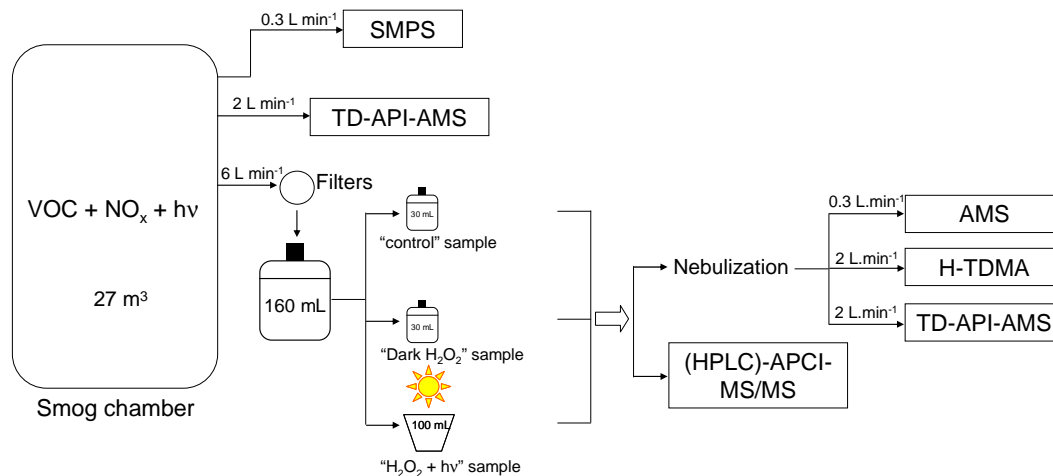


Fig. 1. General scheme of the experiments, including SOA formation in the smog chamber, SOA extraction, aqueous phase processing and nebulization with the instruments used.

Title Page

Abstract

Introduction

Conclusions

References

Tables

Figures

◀

▶

◀

▶

Back

Close

Full Screen / Esc

Printer-friendly Version

Interactive Discussion

Aqueous phase processing of secondary organic aerosols

Y. Liu et al.

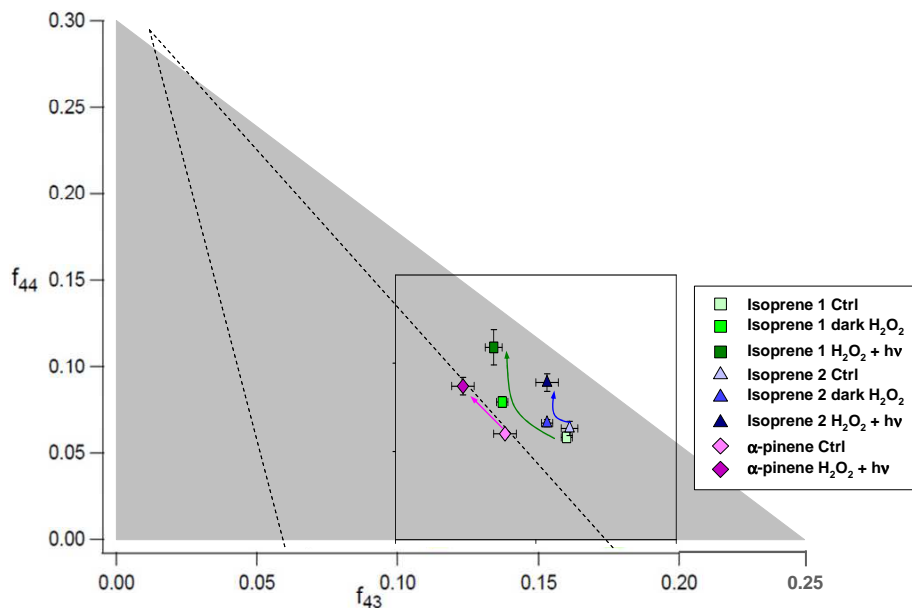


Fig. 2. f_{44} versus f_{43} for LV-OOA and SV-OOA components from a compilation of ambient air data (dotted line area) (Ng et al., 2010) and simulation chamber data (grey area) (Lee et al., 2011), and from isoprene and α -pinene experiments measured in this work. Uncertainty is the standard deviation for the first 45 min of nebulization. Ctrl: “control” samples, dark H_2O_2 : “dark H_2O_2 ” samples and $\text{H}_2\text{O}_2 + hv$: “ $\text{H}_2\text{O}_2 + hv$ ” samples.

Title Page

Abstract

Introduction

Conclusions

References

Tables

Figures

⏪

⏩

◀

▶

Back

Close

Full Screen / Esc

Printer-friendly Version

Interactive Discussion

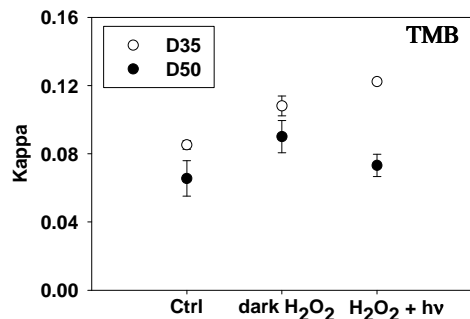
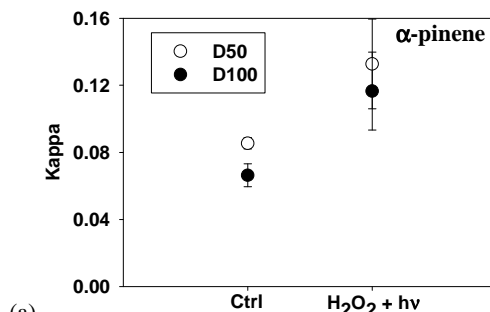
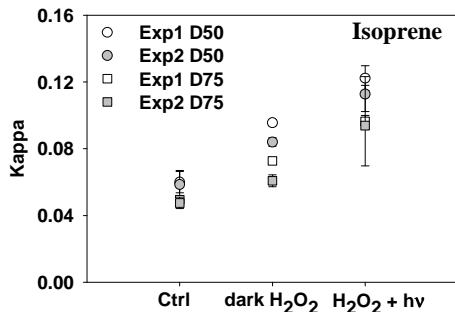


Fig. 3. Hygroscopicity parameter kappa (κ) measured during nebulization of “control” samples (Ctrl), “dark H₂O₂” samples (dark H₂O₂) and “H₂O₂ + hv” samples (H₂O₂ + hv) for isoprene **(a)**, α -pinene **(b)** and TMB **(c)** experiments. The kappa values were measured on 50 nm and 75 nm dry particle diameters D_{50} , D_{75} for isoprene; on 50 nm and 100 nm dry particle diameters for α -pinene; and on 35 nm and 50 nm dry particle diameters for TMB. Error bars represent the standard deviations during 90 min of nebulization (for TMB of process sample, only one value was measured at 35 nm).

Aqueous phase processing of secondary organic aerosols

Y. Liu et al.

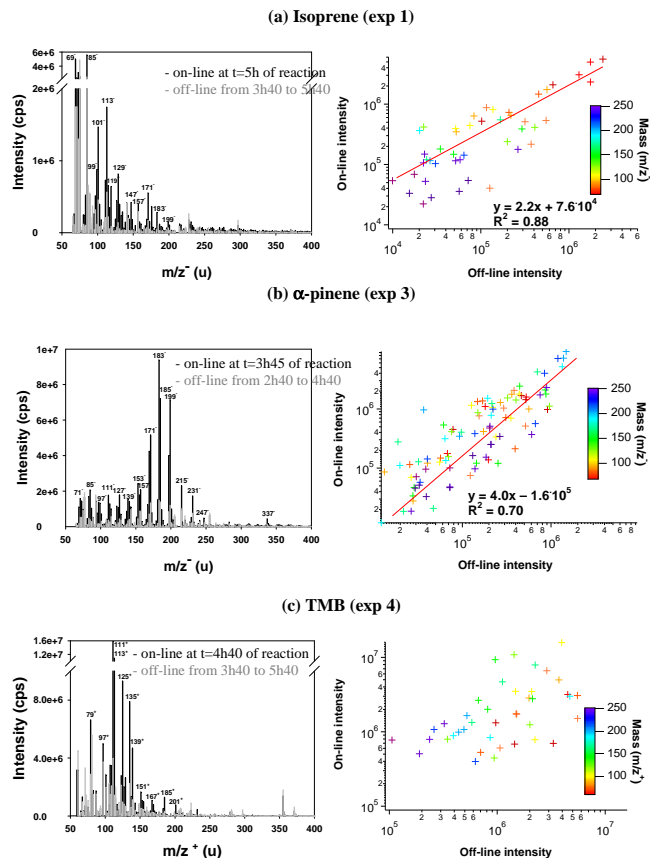


Fig. 4. TD-API-AMS measurements of the chemical composition of SOA formed during the photooxidation and correlation between on-line and off-line analysis of (a) isoprene (b) α -pinene and (c) TMB. Comparison of the mass spectra obtained (i) in black: by direct on-line measurement in the smog chamber at time t after lights on; and (ii) in grey: by nebulization of “no process” samples.

Title Page

Abstract

Introduction

Conclusions

References

Tables

Figures

◀

▶

◀

▶

Back

Close

Full Screen / Esc

Printer-friendly Version

Interactive Discussion

Aqueous phase processing of secondary organic aerosols

Y. Liu et al.

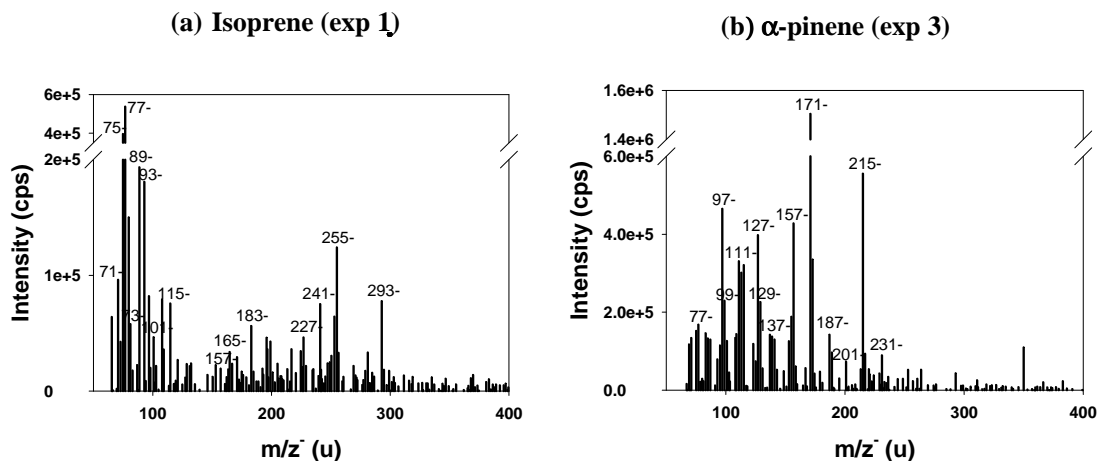


Fig. 5. Mass spectra differences between $\text{H}_2\text{O}_2 + h\nu$ samples and “control” samples which show the ions formed during the aqueous phase processing for isoprene **(a)** and α -pinene **(b)**, measured with APCI-MS by direct injection of aqueous solutions.

[Title Page](#)[Abstract](#)[Introduction](#)[Conclusions](#)[References](#)[Tables](#)[Figures](#)[◀](#)[▶](#)[◀](#)[▶](#)[Back](#)[Close](#)[Full Screen / Esc](#)[Printer-friendly Version](#)[Interactive Discussion](#)

Aqueous phase processing of secondary organic aerosols

Y. Liu et al.

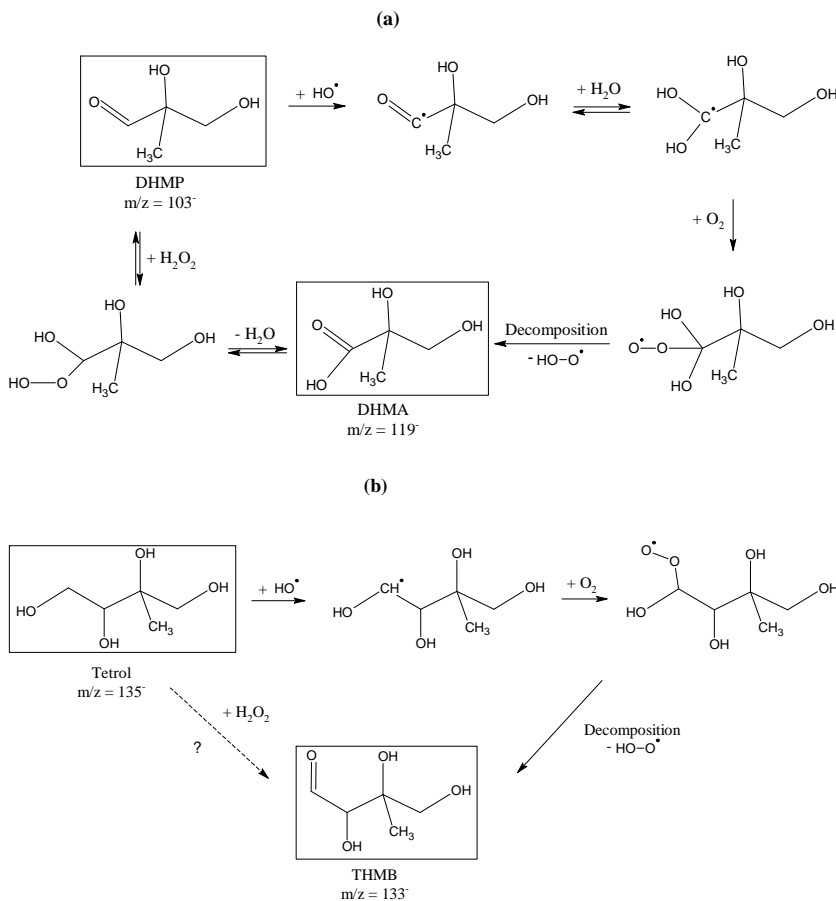


Fig. 6. Chemical mechanism of aqueous phase oxidation by H_2O_2 and by OH radicals of **(a)** 2,3-dihydroxy-2-methyl-propanal (DHMP) leading to 2,3-dihydroxy-methacrylic acid (DHMA); and **(b)** 2-methylbutane-1,2,3,4-tetrol (tetrol) leading to trihydroxy-3-methylbutanal (THMB).

Title Page

Abstract

Introduction

Conclusions

References

Tables

Figures

◀

▶

◀

▶

Back

Close

Full Screen / Esc

Printer-friendly Version

Interactive Discussion

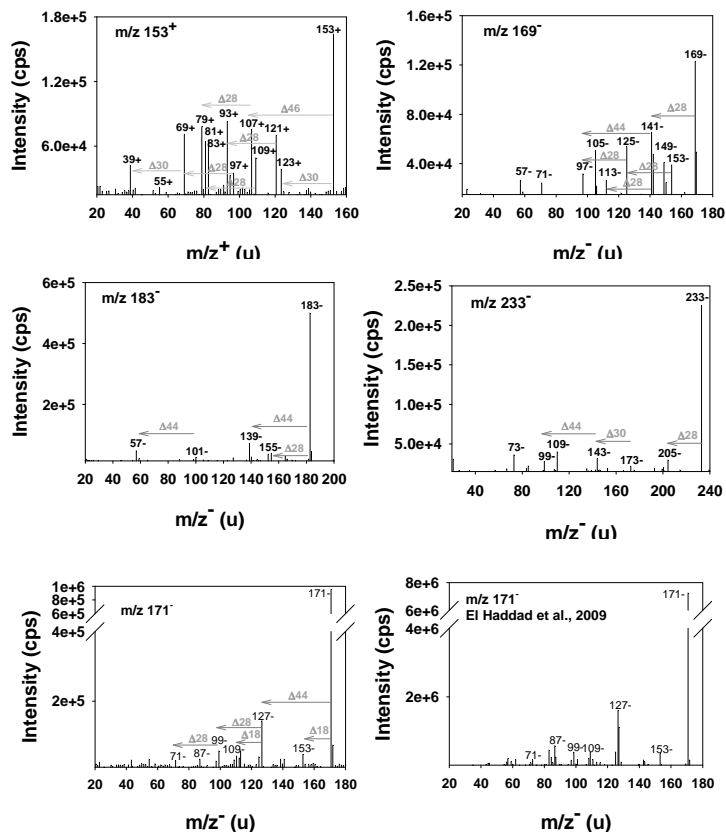


Fig. 7. APCI-MS² spectra of five reaction products observed in “H₂O₂ + hν” sample after isoprene photooxidation (exp. 2) in the mass range 150–300 amu. The fragmentation spectrum obtained for $m/z = 171^-$ (collision energy = 10 eV) is compared to the one obtained by El Haddad et al. (2009) during the aqueous phase photooxidation of methacrolein (collision energy = 8 eV) (at 20 h of reaction), which is one of the major gas-phase reaction products of isoprene.